

Exploration of quiescent plasma for wave studies in MPD

Meenakshee Sharma^{1,2}, A. D. Patel¹, N. Ramasubramanian^{1,2}, Y. C. Saxena¹, P. K. Chattopadhyaya^{1,2}, and R. Ganesh^{1,2}

¹*Institute for Plasma Research, Bhat Gandhinagar-382428*

²*Homi Bhabha National Institute, Anushakti Nagar, Mumbai-400094*

Abstract

A Multi-pole line cusp Plasma Device (MPD) built using six electromagnets is capable of producing six pole six magnets (SPSM) and twelve pole six magnets (TPSM) cusp configuration. In this article, a detail experimental study of the plasma parameters in these two multi-pole line cusp geometries is presented. SPSM has very small field free region (extending upto $R \sim 4$ cm) compared to TPSM (which extends upto $R \sim 10$ cm). The radial variation of plasma parameters for various, magnetic field strengths, is presented. The uniformity in radial and azimuthal variation of plasma parameters is observed to be comparable to the radial extent of field free regions in both cusp configurations. The variation is $<5\%$ upto $R \sim 4$ cm and $R \sim 10$ cm in SPSM and TPSM respectively. The plasma is quiescent over a larger volume for TPSM ($\delta n/n < 0.1\%$) compared to SPSM. The experimental investigation of plasma parameters in SPSM and TPSM provides very strong evidence that the magnetic field profiles of cusp magnetic field configuration play a crucial role in determining the uniformity of plasma parameters and plasma quiescence level. The different aspects of wave excitation in plasma can be studied in the background of this enhanced volume of plasma uniformity and quiescence in TPSM.

I. Introduction

The production of large volume, uniform and quiescent plasma has been a subject of research since many decades because of its various applications, such as material plasma processing [1–8], plasma wall interaction for material selection plasma facing component in ITER [9], used in thermonuclear fusion also due to the favorable magnetohydrodynamic stability [10–13]. Limpaecher and MacKenzie [14] first showed that multipole cusp magnetic field could be used to produce such plasma with enhanced densities. Such magnetic field enhance the plasma density ~ 100 times and also make the plasma more quiescent and uniform (Leung *et al* 1983, Bacal *et al* 1985, Holmes *et al* 1985). The energetic ionizing electrons are confined in the plasma by the magnetic fields at the walls resulting in a high ionization efficiency [15]. Because of the quiescence nature, the plasma confined by multipole magnetic field has also been found to be useful for studies of fundamental plasma phenomenon, such as study of excitation and propagation of various waves in plasma, wave particle trapping and un-trapping, Landau damping of waves, phase mixing and wave breaking.

The Multi-pole line cusp Plasma Device (MPD) [16] has adopted this multi-pole line cusp magnetic field geometry for plasma confinement. The usage of electromagnets in MPD facilitates the confinement of plasma with various cusp geometries and a wide range of magnetic field strengths. The characteristics of the filamentary produced argon plasma has been studied and reported before [16,17]. In the edge region of the six pole line configurations, drift waves have been observed [18], while in the central region the plasma is very quiescent. This quiescent and uniform plasma volume of the central region can be used for fundamental plasma phenomena studies as well as plasma applications as mentioned above. To further increase this quiescent and uniform plasma volume, 12-pole line cusp configuration was studied, by passing current in the same direction in all electromagnets. It was found that this 12 pole configuration is more advantageous and has been used to study the propagation of perturbing voltage pulses with frequencies in the ion acoustic range [19]. This article, reports the detailed plasma characteristics in the Twelve Pole Six Magnet (TPSM) configuration as compared to the Six Pole Six Magnet (SPSM) configurations. The rest of paper is organized as follows, the schematic of the device and diagnostics are described in Section II, and Section III contains the experimental observations followed by discussion and a brief summary in section IV.

II. Experimental Setup and Diagnostics

i. Plasma production

The experiments reported here are performed in a linear cylindrical device MPD, which has been described before [16,17] and schematic of the MPD and its diagnostics in Figure 1. The device has a cylindrical chamber of 150 cm length and 40 cm diameter and 0.6 cm thick wall made of stainless steel. The system is pumped down to 2×10^{-6} mbar base pressure and the operating pressure of filled Argon gas varies from 5×10^{-5} mbar to 3×10^{-3} mbar. A rectangular filamentary array of $8 \times 8 \text{ cm}^2$, centered at $R=0 \text{ cm}$, is used as cathode to produce the plasma. The filaments are heated for thermionic emission of electrons using a 15V, 500A floating power supply biased at -50V with respect to anode (wall of the cylindrical chamber) using 128V, 25A power supply.

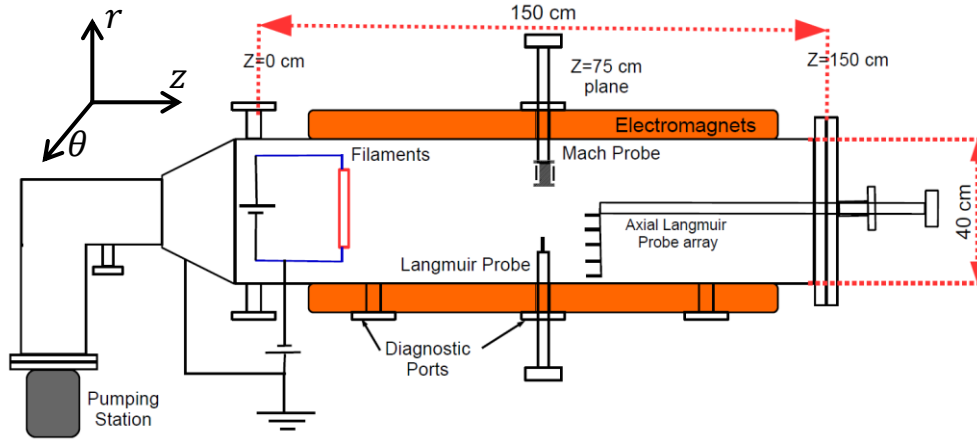


Figure 1: Schematic of side view of the MPD device, electromagnet and its diagnostics, inset of the figure shows the opted coordinate system of the device. All the measurements have been performed on $z = 75$ plane.

Confinement of Argon plasma is provided by 6 axis-symmetric 120 cm long cylindrical bars of vacoflux embedded in copper coils as shown in figure 2. The electromagnets are spaced every 60 poloidal degrees on the periphery of the cylindrical main chamber pointing radially inward. The resulting magnetic cusps are cylindrically symmetric in the poloidal direction.

ii. Magnetic field configuration

Use of electromagnets in MPD, gives us flexibility to work with different multi-cusp geometries by just changing the direction of current in electromagnets and a wide range of magnetic field strength allows us to monitor the change in plasma parameters with magnetic field geometry and

strength. The direction of current in these electromagnets decides the North (N) and South (S) poles of each magnet. Various cusp geometries can, thus be produced and in this paper we present results from two cusp geometries, one produced, when current in all the six electromagnets passes in the same direction, and other by passing currents in alternate magnets in opposite directions. In the first configuration, the current in same direction produce six North poles on the inner circumference of the cylindrical device.

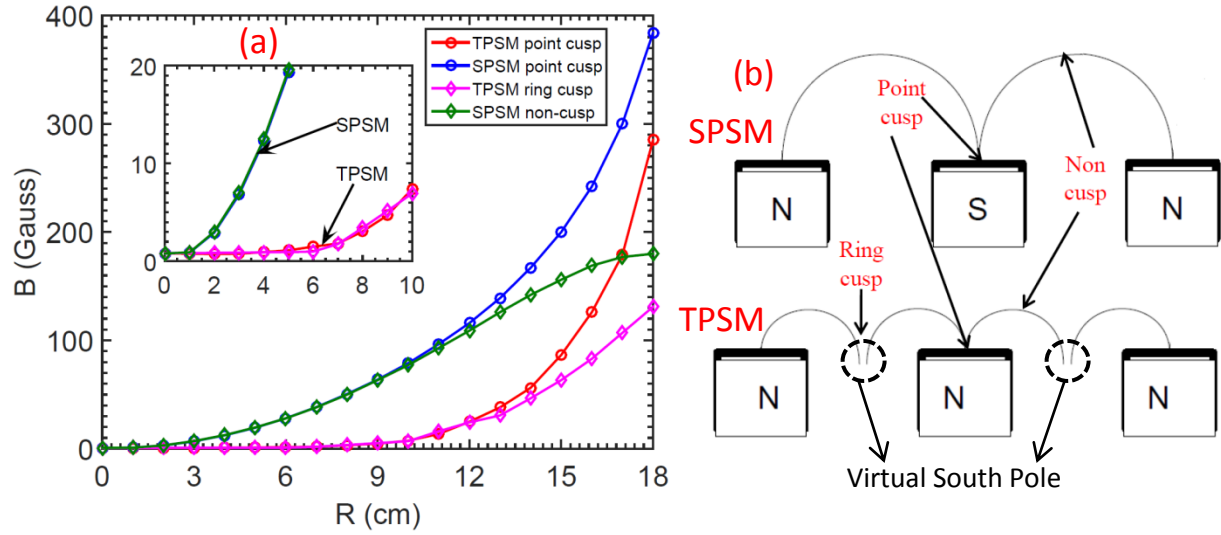


Figure 2: Radial variation of magnetic field strength for twelve pole six magnet (TPSM) and six pole six magnet (SPSM) cusp configuration. The region from center of the device to pole of the magnets radially outward is point cusp and the region from center of the device to exactly middle of the pole of the magnets is ring cusp in TPSM and non-cusp in SPSM. Figure (b) shows the schematic of SPSM and TPSM. The point cusp (the region from center of the device to pole of the magnets), non-cusp (the regime from centre of the device to exactly middle of the two pole surface), and ring cusp regimes (the regime from centre of the device to virtual pole occurs only in TPSM).

As shown in figure 1(b) the field lines converge on the north poles and in between two like poles the field lines go parallel to each other, this creates a resemblance of virtual south poles at the inner circumference of the device. In this configuration, there is six north poles and six virtual south poles, hence it is named as Twelve Pole Six Magnet (TPSM) Cusp Configuration. In the second configuration the current in alternate direction produce alternate North and South poles on the inner circumference of the cylindrical device. In this arrangement, the field lines emerging from one North Pole terminate on adjacent South poles and create a continuous field lines, as shown in figure 2(b), there are six poles (3-north, 3-south) and it is named as Six Pole Six Magnet (SPSM) Cusp Configuration. The region from center of the device to pole of the

magnets, radially outward named as point-cusp region in both magnetic field configurations, where the field lines converge or diverge. The region from center of the device to middle of the two pole surfaces is named as non-cusp region, in SPSM it is exactly in between two magnets and in TPSM it lays in between north pole and virtual south pole. Similarly, the region from center of the device to virtual pole is named as ring cusp and it occurs only in TPSM. The detail schematic of all these cusp regimes is shown in figure 2(b). Radial profile of magnetic field for both cusp configurations is shown in figure 2(a). The radial variation of magnetic field shows that the field value is less than 10 Gauss upto 10 cm for TPSM and 4 cm for SPSM respectively, indicating that TPSM has larger field free volume than SPSM.

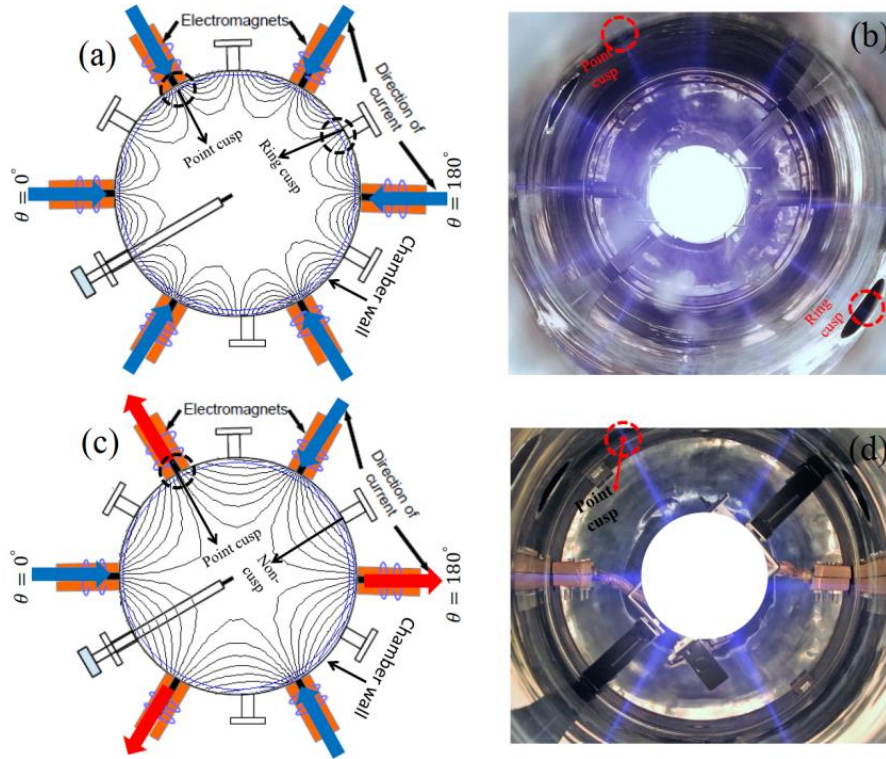


Figure 3: (a) and (c) shows the arrangement of electromagnets over the chamber, diagnostic ports, Langmuir probe for diagnostic and magnetic field lines simulated using FEMM in TPSM and SPSM respectively. Arrow in figures shows the current direction in electromagnets. Figure (b) and (d) shows the pictures of plasma confined in full line cusp configuration (SPSM) and broken line cusp configuration (TPSM) taken through view port from one end of the device.

The magnetic field at pole depends on the current passed in the electromagnets and it is same for SPSM and TPSM, therefore, there exist sharp gradients in magnetic field in TPSM point cusp region as compared to that in SPSM point cusp. Cusp magnetic field produced by 6-electromagnets is symmetric in all r , θ , and z plane, the details of this are discussed before {REF

Amit thesis}. Figure 3(a) and 3(c) shows the simulated cusp magnetic field using FEMM, it also shows the alignment of electromagnets over the outer periphery of the chamber at any z-plane. The images of plasma are taken from a view port placed at one end of the device show the plasma behavior in SPSM and TPSM [figure 3(b) and figure 3(d) respectively]. Plasma produced in the low magnetic field volume follows the field lines and drifts radially outward towards the wall. Here it is channelled into thin loss areas, terminating on the inner wall of the chamber, as shown by plasma images presented in figure 3(b) and 3(d). We can observe from figure 3(a, c) and figure 3(b, d) that plasma confined in these cusp magnetic field exactly replicates the cusp magnetic field profile.

iii. Plasma diagnostics

Argon plasma in both the configuration is characterized by Langmuir probe of 1 mm diameter and 5 mm and used to measure the electron temperature (T_e), plasma density (n), plasma potential (V_p), floating potential (V_f) and fluctuation in plasma density using standard Langmuir probe technique. The probe voltage is swept from -80 V to +25 V and the probe characteristics are examined.

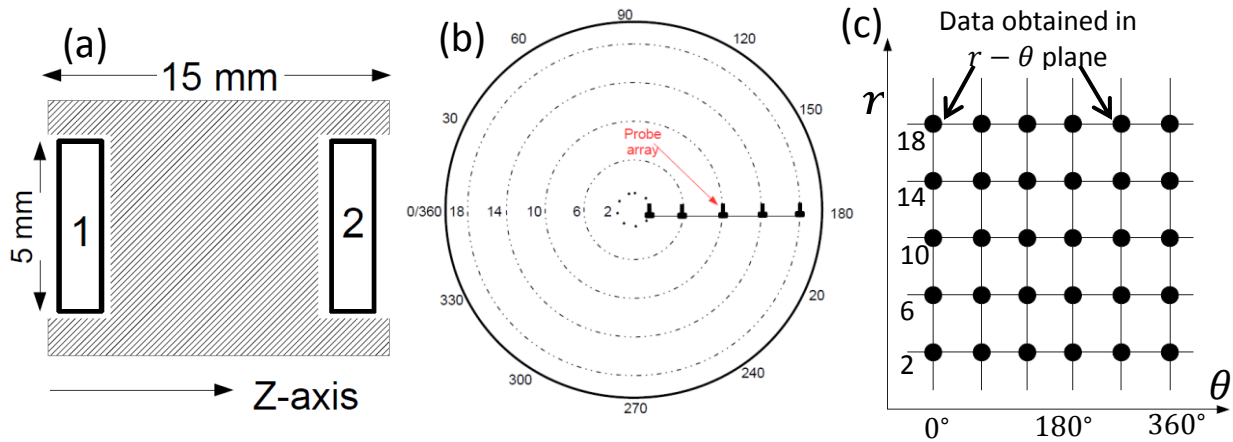


Figure 4: Schematic of (a) Mach probe, (b) five radial probe array integrated with rotatable axial shaft, (c) 2-d measurement in $r - \theta$ plane.

Mach probe, a pair of two disk probes of 5 mm diameter is mounted as per the arrangement shown in figure 4(a). Probe 1 and 2 are front collector and back collector in the direction of z-axis respectively. It is used to determine the radial profile of axial plasma flow. Both probes are biased to negative potential to measure ion saturation current and using the values of ion

saturation current we calculate the Mach number (u_n). The flow can be calculated using Mach number and ion acoustic velocity measured by Langmuir probe, $V_d = u_n C_s$.

A cylindrical device has r, θ , and z co-ordinates as shown in the inset of figure 2. Experimental measurement performed along r is radial variation, along z is axial variation and along θ is known as azimuthal variation. One more diagnostic is established to measure the azimuthal variation of ion saturation current to determine the uniform plasma area. It is a probe array of 5 Langmuir probes placed at five radial locations such as, $R=2, 6, 10, 14$, and 18 cm, each 4 cm apart as shown in figure 4(b). It is 2-d measurements as shown in figure 4(c). This probe array is integrated with a shaft and inserted inside the chamber through the end plate of device, at $R=0$ cm and can be rotated around the center. Therefore, we can perform the azimuthal measurement at various angular locations. It is a 2-d measurement and if we plot this 2-d $r - \theta$ plane as shown in figure 4(c) then the dark circle will be locations data is obtained. In this way we can measure the ion saturation current at all cusp regimes varying from point cusp, ring cusp to point cusp. We can compare the plasma characteristic and nature of fluctuation in different cusp regimes, rarely reported in earlier work carried in cusp magnetic field devices. The details of experimental results are discussed in the following section III.

III. Observations

The plasma parameters for the both the configurations are measured at vertical mid plane of the device, which is $Z = 75$ cm for 2×10^{-4} mbar Argon pressure and -50 V discharge voltage to create the same background plasma conditions. A detail experimental observation of plasma characteristics in SPSM and TPSM is reported in this section, which includes variation of plasma parameters with increasing magnetic field strength at $R = 0$ cm, azimuthal variation of ion saturation current, radial variation of plasma parameters, plasma quiescence level, and axial plasma flow for pole magnetic field $B_p = 800$ Gauss, axial plane $Z=75$ cm, Argon pressure 2×10^{-4} mbar and -50 V discharge voltage.

A. Characterization of Mean Plasma Parameters

i. *Variation of Plasma Parameters with Cusp Magnetic Field Strength at the center of MPD*

The variation of plasma parameters with increasing cusp magnetic field strength measured at $R=0$ cm for both the cusp magnetic field configuration are shown in figure 5. The line with circle and line with diamond shape marker shows plasma parameters for TPSM and SPSM respectively. Figure 5(a) shows the variation of floating potential (V_f), the value of floating potential is relatively more negative in SPSM compare to TPSM for all magnetic field values. It indicates higher confinement of hot electrons in SPSM relative to TPSM. This can also be confirmed from figure 5(b), which shows the relative hot electron population for both cusp configurations. The hot electrons density relative to plasma density, $(n_{eh}/n) \times 100$, varies from 0.7% – 1.5% in SPSM and 0.07% – 0.8% in TPSM; nearly twice in SPSM. It indicates the full cusp can confine the same amount of hot electrons in very less magnetic field. As reported earlier [17] it is seen that as the cusp field strength increases the leak width of plasma (plasma loss to the chamber wall while following the field lines) decreases and as a consequence the hot electron population increases. This leads to increase in magnitude of plasma density. Plasma density in both cusps increases with increase in the cusp magnetic field strength as shown in figure 5(c). Though the confinement of hot electrons is higher in SPSM compare to TPSM as shown by figure 5(a) and 5(b), yet the plasma density is comparable in both cusp configurations for each magnetic field strength. However, the exact cause and origin of the observation of comparable density is not clear, so we shall come back to this point again. The variation of plasma bulk electron temperature, T_{ec} with increasing cusp magnetic field strength is shown in figure 5(d). The bulk electron temperature does not vary much with magnetic field strength and it is nearly same for both TPSM and SPSM. It suggests that the physical mechanism that governs the electron temperature in plasma is likely to be independent of magnetic field. The variation of hot electron temperature, T_{eh} with increasing cusp magnetic field strength is shown in figure 5(e) it does not vary much with magnetic field strength and is comparable for both TPSM and SPSM. The energy of hot electrons depends upon the discharge voltage and neutral density. Both are kept constant at -50 V and 2×10^{-4} mbar for both configurations. Therefore the temperature of hot electrons (hot electrons) does not vary with magnetic field. The plasma potential V_p is also

nearly constant with variation of cusp magnetic field strength in both the configurations, and observed to be same in both the configurations, as shown in figure 5(f).

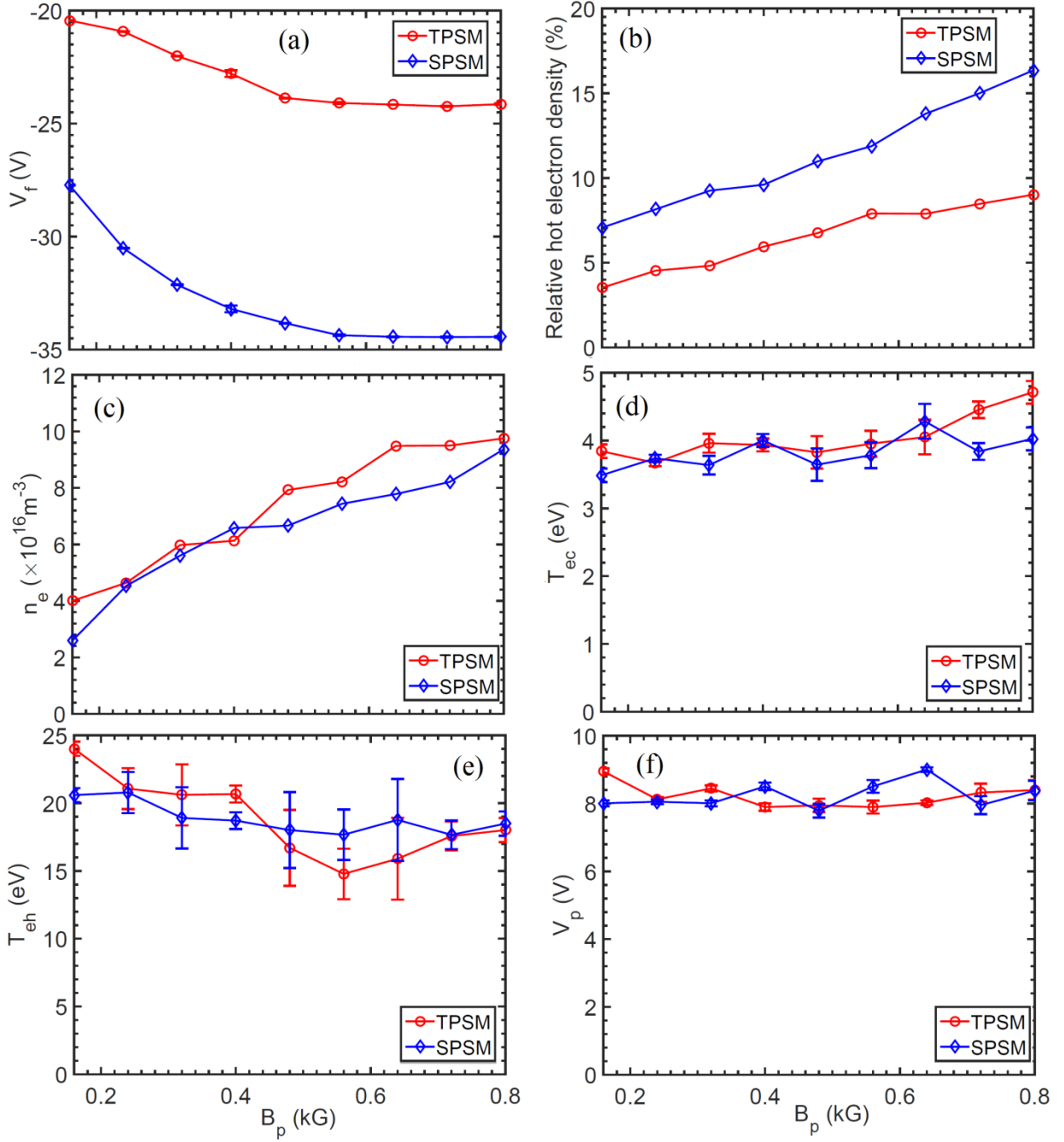


Figure 5: Variation of plasma parameters with various magnetic field strength (a) floating potential, V_f , (b) plasma density, n , (d) hot electron density, n_{eh} , (c) temperature of bulk electron, T_{ec} , (e) temperature of hot electron, T_{eh} , and (f) plasma potential, V_p measured at $R=0$ cm, for full line and broken line cusp configuration (SPSM and TPSM) at 2×10^{-4} mbar pressure and -50 V discharge voltage.

It can be observed from the figure 5 that confinement of hot electron is more in SPSM compared to TPSM and all other plasma parameters, plasma density, electron temperature, plasma potential and floating potential shows comparable values in both cusp configurations and follows the similar profile with increasing cusp magnetic field strength. Taking this observation one step ahead in next section III B, the azimuthal profile is discussed.

i. Azimuthal Variation Ion Saturation Current

The cusp topology contains cylindrical symmetric and this argues that at any particular z-plane the area of $\sim 10\text{cm}$ and $\sim 4\text{cm}$ radius is field free area in TPSM and SPSM respectively. Due to the cylindrical symmetry, at any z-plane the radial profile of both cusp magnetic fields will be same at all angular or azimuthal planes. The 6-electromagnets are arranged on the outer periphery of main chamber each 60° apart. If we assume one of the electromagnet at $\theta = 0^\circ$, then others will be at 60° , 120° , 180° , 240° , and 300° . The terminology of point cusp, ring cusp and non-cusp stands as discussed earlier in section II, hence, we can say that, all azimuthal magnet locations are point cusp regimes in both cusp configuration. The probe with multiple array is used to measure the azimuthal variation of ion saturation in both cusp configuration, obtaining the at all point, ring and non-cusp regimes, at $Z=75\text{cm}$ plane. The measured profile of azimuthal variation of ion saturation current is shown in figure 6(a) and 6(b) for TPSM and SPSM respectively. In TPSM, there are 6-point cusp, 6-ring cusp and 12-noncusp regimes and the data is obtained at 24 azimuthal planes, as shown in figure 6(a). In SPSM, there are 6-point cusp regimes and 6-noncusp regimes and the data is obtained at 12 azimuthal planes, as shown in figure 6(b). The ion saturation current is measured at five radial locations. We can observe in figure 6(a) that in TPSM at $R=2, 6, \text{ and } 10\text{ cm}$, values of ion saturation current do not vary with variation of azimuthal planes from point cusp to ring cusp to non-cusp. The change in cusp topology does not affect the ion saturation current upto area of 10 cm radius. After 10 cm , at $R=14\text{cm}$ and 18cm we can observe that the ion saturation current is higher in point and ring cusp and falls down in non-cusp regime. Even at $R=14$ and 18 cm the values of ion saturation current are nearly same in ring and point cusp. Now if we observe the figure 6(b), that in SPSM only at $R=2\text{ cm}$ the values of ion saturation current do not changes with variation of azimuthal planes from point cusp to non-cusp. After $R=2\text{cm}$, at all radial locations ion saturation current possess higher value in point cusp regimes and falls down in non-cusp regimes.

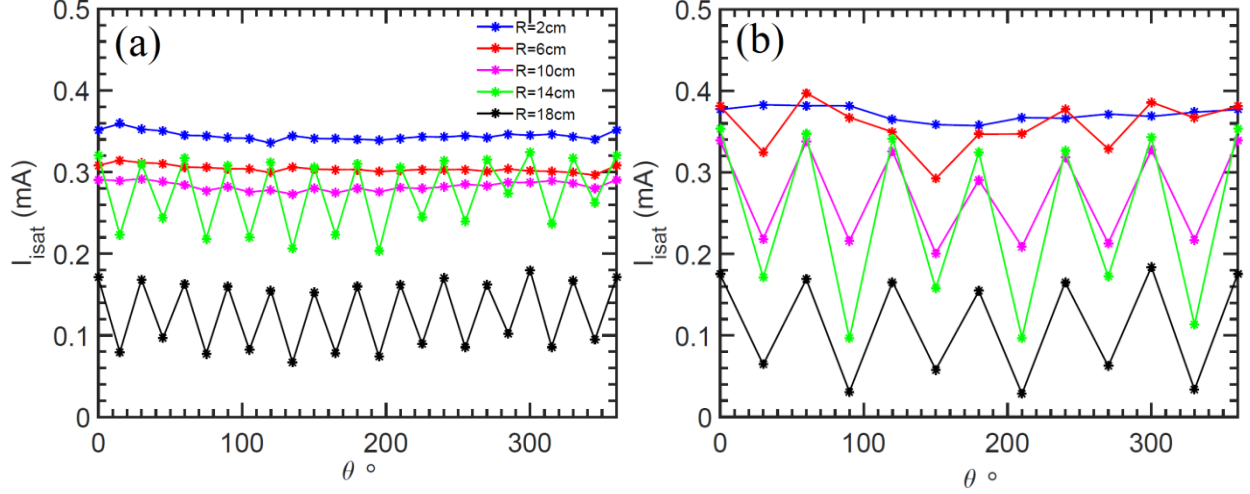


Figure 6: Azimuthal variation of ion saturation current (a) in TPSM, and (b) SPSM for five radial location $R=2, 6, 10, 14$, and 18 cm , measure at $Z=75\text{ cm}$, mid plane of the device for $2 \times 10^{-4}\text{ mbar}$, -50 V discharge voltage and $B_p = 400\text{ kG}$.

From figure 6, we can deduce that the value of ion saturation current is higher in point cusp (ring cusp also in TPSM) compare to non-cusp regime. In TPSM, larger uniformity is observed, upto $\sim 10\text{cm}$, compare to SPSM ($\sim 2\text{cm}$) without the effect of cusp magnetic field topology, since the magnetic field profile also shows the field free region upto similar extends. The decrease in ion saturation current from point cusp to non-cusp is observed to be larger in SPSM than it is in TPSM. Hence the azimuthal profile suggests that the gradient in ion saturation current from point cusp to non-cusp is very weak in TPSM compare to SPSM. Using the probe array, data can be obtained at only five radial locations, so to get the complete and more precise radial profile of all plasma parameters, the Langmuir probe inserted in a radial port is used and the observations are discussed in the following section.

ii. Radial Variation of Plasma Parameters

The radial measurement is only possible in between two consecutive magnets, due the limitation of the device and the location of the radial measurements is also shown in figure 3(a) and 3(c). As shown in the figures this location is ring cusp regime in SPSM and non-cusp regime in TPSM. The radial profiles of plasma parameters for plasma immersed in SPSM and TPSM for $B_p = 800\text{ Gauss}$ is shown in figure 7, B_p is value of magnetic field near the pole of the magnet. The radial profiles of plasma density shown in figure 7(a), is measured for non-cusp (five point measurement by axial probe array) and ring-cusp regime (radial Langmuir probe) of TPSM and non-cusp (radial Langmuir probe) and point-cusp regime (five point measurement by axial

probe array) of SPSM. The plasma density is nearly constant and varies $< 5\%$ upto $R \sim 10$ cm for TPSM which corresponds to the respective field free region in the very same configuration. Beyond this the plasma density gradually decreases towards the chamber wall. The density has a sharper gradient for SPSM non-cusp as compared to TPSM. Other plasma parameters presented in this section and figure 7 are measured for TPSM only. Figure 7(b) shows the radial variation of electron temperature, it suggest that the bulk electron temperature is nearly constant upto $R=12$ cm and then has a shallower gradient around $R=12-14$ cm.

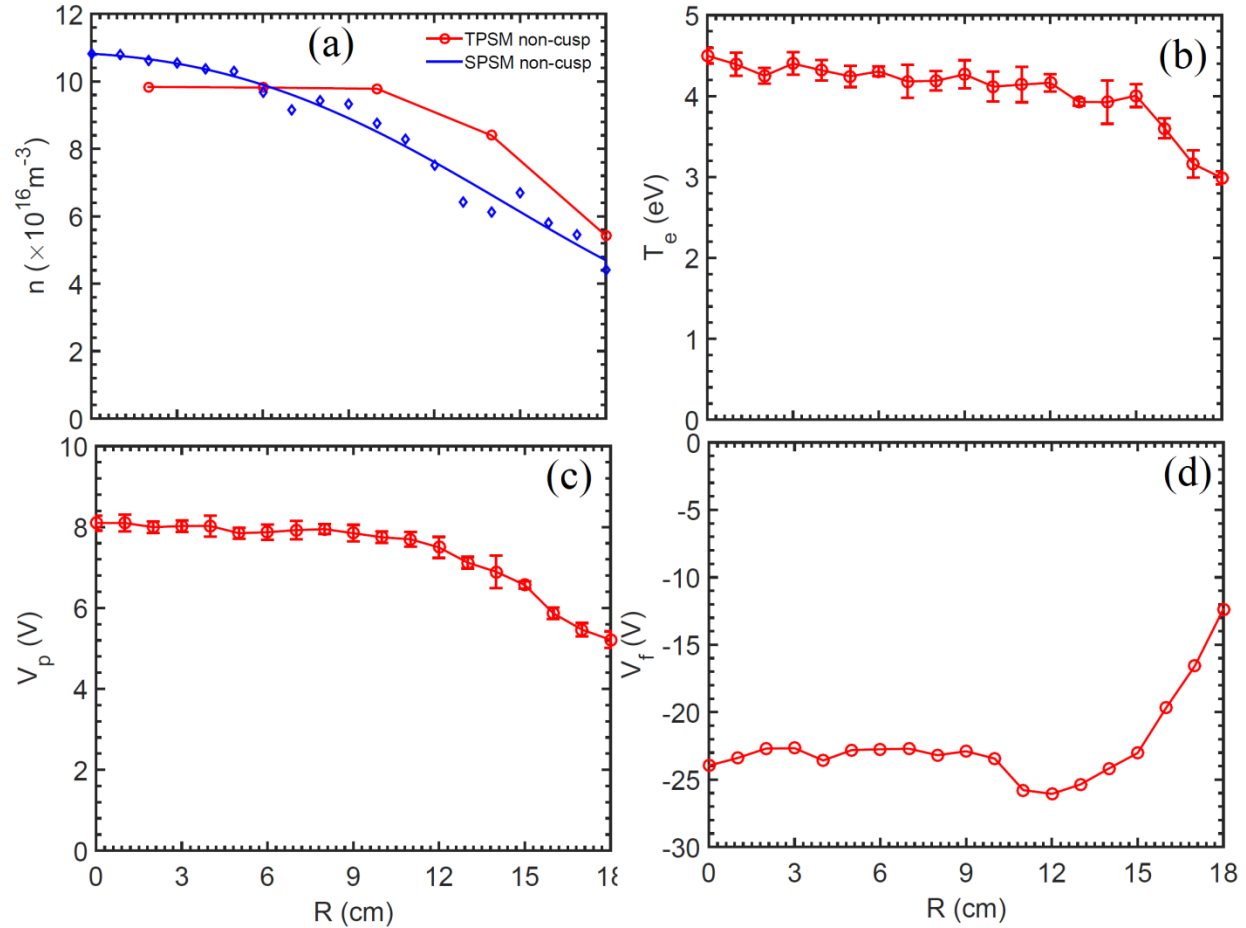


Figure 7: Radial variation of (a) plasma density, n , (b) bulk plasma electron temperature, T_e , and (c) plasma potential, V_p and (d) floating potential, V_f , for $B_p = 800$ Gauss, 2×10^{-4} mbar neutral pressure, and -50 V discharge voltage. The line with circle is for TPSM and line with diamond shape marker is for SPSM.

The plasma potential, as shown in Figure 7(c), is nearly constant and positive up to $R \sim 12$ cm and has a slow gradient outboard. It argues that radial electric field is either not present or it is very feeble. As shown in figure 7(d), the plasma has higher negative value of floating potential (~ -20 V) at $R=0$ cm. It is nearly constant upto $R \sim 10$ cm and approaches to a more negative

value around $R \sim 12 - 14$ cm and it again reaches to less negative afterwards with a slower gradient. After reviewing the observation of radial profiles of plasma density in both cusps, we can say that plasma confined in TPSM is more uniform compare to SPSM. Here we have discussed the radial uniformity of plasma parameters and observed that in TPSM the density has more uniform area. Any signature of electric field, temperature and floating potential is also constant in that area.

B. Characterization of Plasma Fluctuations

i. Quiescence Level

The level of fluctuation in plasma density is measured for both configurations and radial variation is shown in figure 8, the line with circle is for TPSM and line with diamond shaped marker is for SPSM.

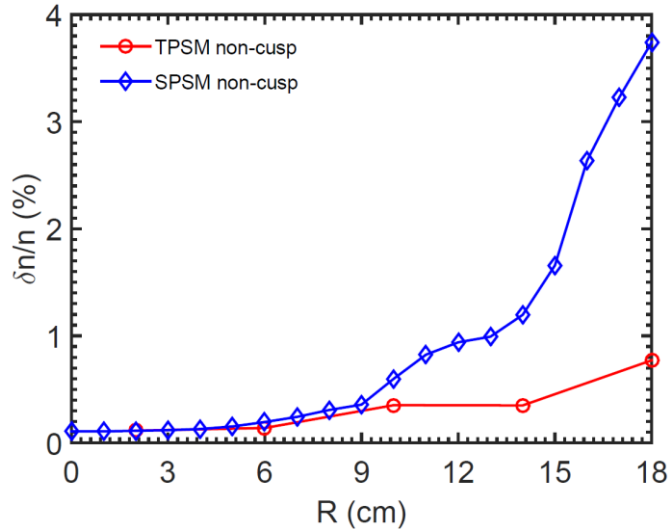


Figure 8: Radial variation of level of fluctuation in plasma density measured for pole cusp magnetic field $B_p = 800$ Gauss, 2×10^{-4} mbar neutral pressure and -50 V discharge voltage. The line with circle is for TPSM and line with diamond shape marker is for SPSM.

The figure 8 shows the comparable low ($< 0.1\%$) values of level of fluctuation in density for both configuration upto radial extent of $\sim 4 - 5$ cm. The level of fluctuation in SPSM increases radially outward from $R \sim 4 - 5$ cm, rising sharply near to wall of the device. The level of fluctuation in TPSM has a constant low ($< 0.1\%$) values upto $R \sim 14$ cm rising to $\sim 0.8\%$ towards wall of the device. We can observe that the radial profile of density fluctuation follows the radial

profile of plasma density in both cusps. The radial extent where the plasma density variation is uniform and $<5\%$, the density fluctuation is $<0.1\%$ and uniform. The value of level of fluctuation near to chamber wall at $R = 18$ cm is relatively very less in TPSM ($\sim 0.8\%$) than SPSM ($\sim 4\%$). In broken cusp the level of fluctuation is less than 1% throughout the radial extent. Any instability present in plasma can cause the increase in fluctuations in SPSM or vice versa is also possible.

A detail study of density fluctuation in SPSM near to wall is reported before [18], in which the presence of drift wave due to gradient in plasma density is observed in non-cusp regime. The same experiments are carried out in non-cusp regime of SPSM and TPSM to determine the nature of fluctuations and presence of the drift wave mode.

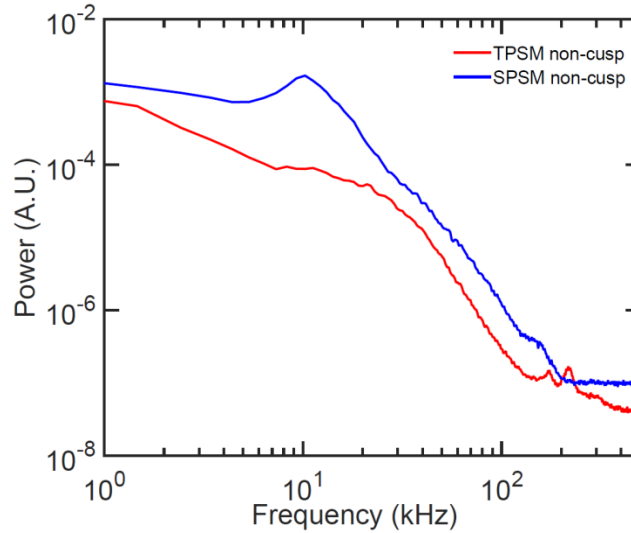


Figure 9: Auto-power spectrum of density fluctuation at $R = 14$ cm, for pole cusp magnetic field $B_p = 800$ G when magnets are energized with magnet currents 100 A.

The spectral analysis is performed with the measured signals of density fluctuations. The auto power spectra of density fluctuation, measured at $R=14$ cm in non-cusp regime of both configuration, is presented in figure 9, for pole magnetic field $B_p = 800$ G. The figure shows a peak in the range of 10 kHz for SPSM case showing the presence of drift wave and no signature of drift wave is present in TPSM. The same measurement is performed in the point cusp of both configurations and ring cusp of TPSM and no signature of drift wave are observed in cusp regimes. It can be argued from the radial profiles of plasma density and azimuthal profile of ion saturation current that the gradient in the profiles of TPSM is relatively very weak to excite any gradient driven fluctuation, like the drift wave observed in SPSM.

ii. Axial Plasma Flow

The net axial plasma flow (V_d/C_s) is measured using Mach probe the results are shown in figure 10. It suggests, that the net axial flow in the centre of the device is negligible $< 0.1C_s$ for the both the cusp configurations. As we move radially outboard the axial flow increases in SPSM and remains constant in TPSM. The net axial flow in TPSM is $< 0.2C_s$ throughout the whole radial extent and in case of SPSM the axial flow increases sharply in outboard regime. The flow driven by drift wave is found along z-axis as reported in earlier work [18] and the driver of the mechanism behind this observation is also discussed. In TPSM the absence of the very same driver leads to negligible axial flow. It shows that, when plasma is confined in TPSM no background axial flow is present.

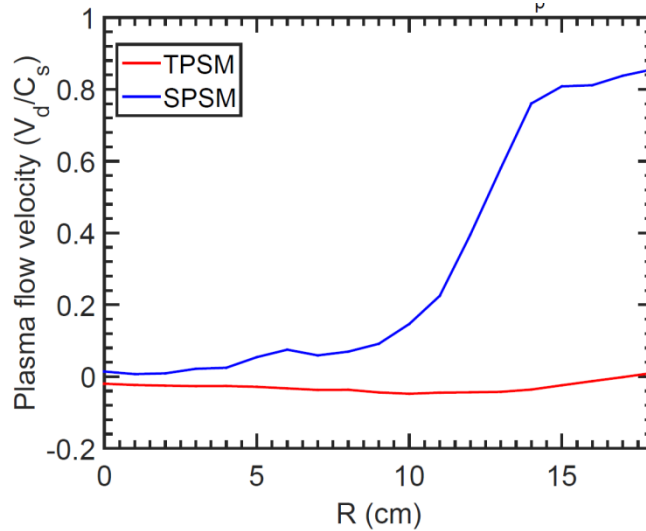


Figure 10: Radial profile of net axial plasma flow measured using the Mach probe, for pole magnetic field $B_p = 800$ G.

IV. Discussion

The main feature of cusp magnetic field is confinement of hot (energetic ionizing) electrons. Hot electrons trapped along the cusp field lines are forced to spend a larger time in plasma. The hot electrons follow the cusp field and get reflected from the magnetic mirror field at the poles of magnets. In this way, they bounce back and forth before escaping to wall. The increase in cusp field increases their path length and flight time. Hence the probability of their collision with neutral gas atom in the plasma also increases resulting in the enhancement of plasma density as

reported earlier too. A simple indicator for the confinement of hot electrons is the enhanced negative value of floating potential in plasma. Enhancement is gauged by an increase in the magnitude of floating potential; it is a direct measurement of hot electrons. The field free central region plays a crucial role determining the volume available for the formation of uniform plasma.

In summary, the observation of variation of plasma parameters in SPSM and TPSM provides very strong evidence that the magnetic field profile plays a crucial role in formation of mean plasma profile, plasma fluctuations and transforming the plasma characteristics. TPSM has larger field free volume and shows more radial uniformity in plasma density with $< 5\%$ variation in the area of circle with $R \sim 10$ cm and $\delta I_{isat}/I_{isat} < 1\%$ throughout plasma. The azimuthal uniformity of area of ~ 10 cm radius, absence of drift wave mode, absence of any background plasma flow and fluctuations makes the ideal plasma background to excite any wave mode or perturbation. The examination of plasma parameters suggests the plasma confined in TPSM is more uniform and quiescent and is the best configuration for fundamental plasma study such as excitation of plasma waves, study of wave-particle interaction, Landau damping etc.

References

- [1] V. N. Tondare, Journal of Vacuum Science & Technology A: Vacuum, Surfaces, and Films **23**, 1498 (2005).
- [2] H. Conrads and M. Schmidt, Plasma Sources Science and Technology **9**, 441 (2000).
- [3] W. L. Stirling, P. M. Ryan, C. C. Tsai, and K. N. Leung, Review of Scientific Instruments **50**, 102 (1979).
- [4] M. A. Lieberman and A. J. Lichtenberg, *Principles of Plasma Discharges and Materials Processing* (John Wiley & Sons, Inc., Hoboken, NJ, USA, 2005).
- [5] S. Mukherjee and P. I. John, Surface and Coatings Technology **93**, 188 (1997).

- [6] R. Günzel, E. Wieser, E. Richter, and J. Steffen, *Journal of Vacuum Science & Technology B: Microelectronics and Nanometer Structures Processing, Measurement, and Phenomen* **12**, 927 (1994).
- [7] T. E. Wicker and T. D. Mantei, *Journal of Applied Physics* **57**, 1638 (1985).
- [8] Y. Wang and T. W. Coyle, *Journal of Thermal Spray Technology* **16**, 898 (2007).
- [9] S. Takamura, *IEEJ Transactions on Electrical and Electronic Engineering* **7**, 1 (2012).
- [10] L. S. Combes, C. C. Gallagher, and M. A. Levine, *Physics of Fluids* **5**, 1070 (1962).
- [11] M. Sadowski, *Review of Scientific Instruments* **40**, 1545 (1969).
- [12] M. G. G. Haines, *Nuclear Fusion* **17**, 811 (1977).
- [13] T. J. McGuire, **1**, (2014).
- [14] R. Limpaecher, K. R. MacKenzie, Rudolf Limpaecher and K. R. MacKenzie, R. Limpaecher, and K. R. MacKenzie, *Review of Scientific Instruments* **44**, 726 (1973).
- [15] K. N. Leung, G. R. Taylor, J. M. Barrick, S. L. Paul, and R. E. Kribel, *Physics Letters A* **57**, 145 (1976).
- [16] A. D. Patel, M. Sharma, N. Ramasubramanian, R. Ganesh, and P. K. Chattopadhyay, *Review of Scientific Instruments* **89**, 043510 (2018).
- [17] A. D. Patel, M. Sharma, N. Ramasubramanian, J. Ghosh, and P. K. Chattopadhyay, *Physica Scripta* **95**, 035602 (2020).
- [18] A. D. Patel, M. Sharma, R. Ganesh, N. Ramasubramanian, and P. K. Chattopadhyay, *Physics of Plasmas* **25**, 112114 (2018).
- [19] M. Sharma, A. D. Patel, Z. Shaikh, N. Ramasubramanian, R. Ganesh, P. K. Chattopadhyay, and Y. C. Saxena, *Physics of Plasmas* **27**, 022120 (2020).

